

Well-Posed Equations of States for Condensed-Phase Explosives

Kibaek Lee,^[a] Alberto M. Hernández,^[a] and D. Scott Stewart^{*(b)}

Abstract: We discuss equation of state forms used to describe condensed high explosive materials that are comprised of mixed components of reactants and products. We show that when the equations of state have poor thermodynamic properties, or good properties but used outside their calibration domain, reactive flow simulations can fail unexpectedly, due to either no states or multiple found thermodynamic states. We propose the use of complete

equations of states for components to build multi-component equations of state for explosive mixtures. Specific examples of equation of state forms are given that show both simulation failure and success, when well-posed equation of state forms are used to simulate blast generated by the initiation of an explosive from an intense high-pressure source.

Keywords: Detonation · multi-component thermodynamics · numerical simulation

1 Introduction

To enable advanced and predictive design of explosive systems, it is important to develop models for high explosive performance that account for realistic chemistry. In particular predictive models minimally must employ a consistent thermodynamic description for explosive reactants and products, if a two-component model is used. As one adds more complexity one requires consistent thermodynamic descriptions for intermediate components as well. Attention to these equation of state details is at the heart of modern (and historically recent) high explosive reactive flow models known as WSD [1] and CREST [2]. We take the use of a thermodynamically consistent framework for multi-component models as an axiomatic starting point for the development of predictive models that can be systematically improved.

We start with the brief description of what is required to build an equation of state model for explosive modeling, and reflect on the current state of the art. The basic problem of detonation has an unreacted material (often at a uniform, quiescent state) ahead of a traveling shock wave that causes the thermodynamic states to jump and initiate chemical reactions in the reaction zone behind the shock. Depending on the length and time scales of observation in a frame that rides with the shock, the chemistry can be quite complex. If one is at the atomistic scale then one has to consider many species and molecular fragments. If one is at the micro-scale that reflects the size of reactant crystallites and or binders in typical manufactured solid explosives, then there is complexity associated with mixing, diffusive burning and transport of many intermediate species. If one considers only the directly measurable states that are experimentally accessible, these are the initial (non-reacting) reactants and presumed completely burnt prod-

ucts. The reactants and products equation of state are calibrated to various shock-based experiments. Both non-reacting reactants, and completely burnt products, are effectively inert and each are idealized as simple materials, but with different enthalpies of formation.

Clearly a detonation model with only two components is a drastic idealization, but its common usage reflects the current state of the art for predictive simulation of the performance of modern high explosives for engineering. However work is underway to include the effects of more chemical components. See for example the work of Vitello *et al.* [3], that uses six components. However, a two component model can predict many aspects of the explosive performance in a high explosive system design. The premise of this paper considers a model with: 1) A minimum set of components, whose isolated components are described by a separate equations of state, (the 2-component model has 2, the 3-component, 3, etc.) 2) A reaction mechanism for change between components that preserves atomic mass (i.e. obeys stoichiometry). 3) A specified equation of state for the mixture of components. Items 1)–3) require a plausible thermodynamic framework and set of assumptions that enables the mathematical closure of the model. Again, the final model specification of the thermodynamic framework depends on the assumed scale of observation.

[a] K. Lee, A. M. Hernández
Department of Mechanical Science and Engineering
University of Illinois, Urbana-Champaign
1206. W. Green St., Urbana, IL 61801, USA

[b] D. S. Stewart
Department of Mechanical and Aerospace Engineering
University of Florida, USA
*e-mail: stewart.dscott@ufl.edu

If one views the mixture on the atomistic scale, to get a continuum formulation one must average the molecular states and identify components in the midst of molecular, vibrational chaos. However one might be able to pose a local phonon temperature and a stress state that reflects local thermodynamics equilibrium. We believe this can be justified at very small scales with the adoption of a single stress and temperature, see Stewart *et al.* [4]. If one were to observe the micro-scale then one might see many resolved hot spots and stress concentrations and might want to consider a theory with multiple temperatures for components and stress dis-equilibrium as well. If one considers a continuum model that accounts for changes on the coarsest (observation) scale that is used to measure the mechanical response of the reactant and product components only, one might be tempted to invoke simple, empirical closure models, such as a pressure equilibrium, volume closure (which leads to two component temperatures), or pressure equilibrium, temperature equilibrium closure, with a single pressure (stress) and temperature for the mixture, see Stewart *et al.* [5]. If one considers the engineering scale models and restricts to only two (or maybe three) components, those models are computationally tractable and can be made predictive. The choice of a single pressure and temperature for a fixed, (defined) composition for the mixture, leads to a classical thermodynamic formulation which is in common use, and is regarded as state of the art.

The processes that occur in the detonation of an explosive takes place on very specific pressure and temperature trajectories, with attendant changes in various major species components. Figure 1 shows a pressure, temperature plane and identifies regions of p, T states that are associated with typical events and processes. For example, if one considers the pressure temperature states generated

by a shock in an unreacted explosive (reactants) for varying shock strengths, one can plot a p, T locus (shown as “Reactant Shock States”). Likewise for a given explosive, one can estimate the states on the Rayleigh line behind the shock for various underdriven and overdriven quasi-steady or steady planar detonation. The p, T states on the Chapman-Jouguet ZND detonation start at the shock (the von Neumann point) and terminate at a complete reaction, sonic state p_{CJ}, T_{CJ} . For example, Figure 1 uses the WSD model for HMX, introduced in Lambert *et al.* [6] and later analysed in Stewart *et al.* [3], to estimate the pressure, temperature loci of the constant volume and energy process and the states realized on the CJ Rayleigh line. One can also estimate p, T regions for other processes like high pressure ambient temperature compression (diamond anvil experiment), shock initiation regimes, and laser and friction ignition regimes that support flames.

We believe that a reasonable engineering model is likely to be most successful, if it can be made consistent with an identified set of reduced components that can be measured by either direct experimental detection or observation in a best practice atomistic simulation. Identification of components allows the postulation of a model reaction mechanism for change between the components. The transition from chemical energy to kinetic and elastic (mechanical potential energy) and thermal energy requires the equation of state of the components (that defines the enthalpies, thermal and energy contributions to each components) and an equation of state for the mixture of the components. We advocate using modern reactive MD simulations that must make accurate predictions of the major components during the decomposition and reaction of the explosive reactants [7,8]. Engineering models can be greatly improved by being informed by and made consistent with the best information available from modern reactive MD.

Multicomponent thermodynamics remains the means to pose a plausible thermodynamic framework that leads to a tractable model in terms of measurable thermodynamic state quantities that are the mixture pressure (or stress), temperature and composition. Complete equations of state are required and in terms of measurable primitive state variables, and this points to the use of the Gibbs potential for any problem that involve phase change or chemical reaction [9]. In the absence of other components (like in the case of pure reactants) the material must be limited to known and measurable properties. Whereas in some thermodynamic formulation phase field variables are used, we argue that one can always replace the phase field variable with a mass fraction or mole fraction that preserves atomic mass. The mass/mole fraction is in fact the physically-based phase field variable and has the property that its use preserves atomic mass during change between components.

Serious problems are often encountered while running real material simulations on typical/routine explosive engineering problems. A simulation will stop or exhibit “strange” behavior when the explosive products and re-

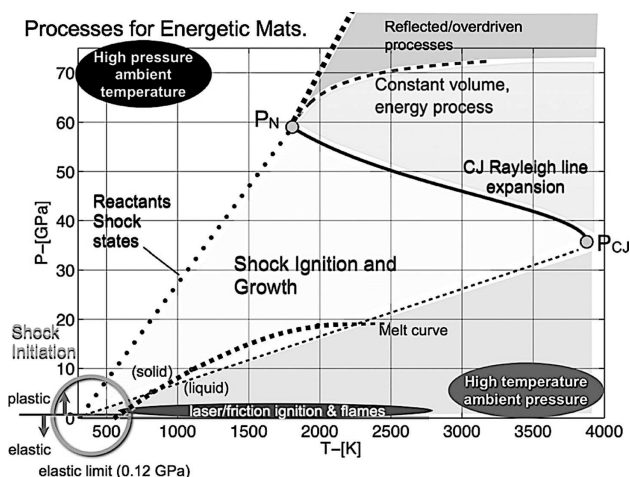


Figure 1. Regions of pressure temperature space, with the expansion process on the CJ Rayleigh line, and the constant volume, energy reaction process as estimated by the Wide Ranging Equation of state model for HMX [3,5].

actants pressure and temperature states are in seemingly stable pressure, temperature domain regions. These symptoms include: negative pressures and densities that lead to estimates of negative sound speed, negative ($T < 0$) or extremely high (unphysical) temperatures that in turn lead to the engineering code's failure to time advance in a simulation. The problems can be traced back to thermodynamic formulations that do not use complete equations of state and/or use temperature as a primitive thermodynamic variable, which in turn leads to an inconsistent thermodynamic framework for the model. The reason incomplete equations of state have been used, are purely historical. If one assumes that the reaction rate for conversion from reactants to products is only dependent on the pressure, then one can avoid using the temperature by assuming that the specific internal energy $e(p, v, \lambda)$ is a function of pressure, specific volume (or density) and reaction progress variable (mass fraction) as the thermodynamic variables. Then temperature is not directly used except for closure and is an auxiliary part of the model formulation. Famous models that have been used with great success include Ignition and Growth [10], but these older models are in the processes of being replaced by models that fully embrace temperature (or equivalently entropy) such as WSD [1] or CREST [2]. The newer models require a complete equation of state.

Section 2 described the multicomponent mixture formulation, identifies the assumptions and reviews how temperature and pressure equilibrium is computed. Section 3 discusses how simulation failure is traced to models for the component equations of state and gives specific examples for commonly modeled condensed explosives. Section 4 describes how one can develop consistent equations of state for the components and the mixtures that can be used for predictive simulation. This includes a brief discussion on how to create tabular equations of state and gives an example where the use of improved EOS description solves the problems that would otherwise be encountered. Finally in the conclusions we discuss how implementing thermodynamically consistent EOS forms improves predictive models for explosive performance and design. Specific details of the EOS forms and parameters are found in the appendix.

2 Formulation for a Multi-component Mixture

For a multi-component mixture we assume that all components are uniformly well-mixed and share one common pressure and temperature. We assume that the material composition is defined by the local mass fractions of the components. The material has (locally) separate pure components in any region where a pure component mixture mass fraction is equal to one. Component (or phase) separation is simply a consequence of the evolution of the mixture during dynamic change. Component volume fractions are computed from the relation between the density and

the mass fraction, and thus can be considered to be auxiliary. The mixture is assumed to have a single mass weighted velocity. For this discussion, transport and viscous dissipation are neglected and the mixture is governed by the compressible Euler equations. The local equilibrium stress tensor that normally appears is replaced by the thermodynamic pressure. We also consider only ideal mixtures and neglect mixture interaction energies. These simplifying assumptions can be relaxed.

Starting from posited Gibbs free energy forms for the components $g(p, T)$, the component volumes are computed from $v = \partial g / \partial p|_T$, which is the volume, pressure, temperature equation of state. This can be inverted to $T = T(p, v)$. Likewise the entropy is computed from $s(p, T) = -\partial g / \partial p|_T$, and the internal energy from $e = g - pv + Ts$ can be rewritten as $e(p, v)$ using the expression for the temperature. The reference energy for each component is usually identified as the enthalpy of formation h_0 at a reference state p_0, T_0 , with $h = e + pv$. The thermodynamic relations hold for the pure component and the mixture. Then (for an ideal mixture), given a mixture with N components the total mixture internal energy and mixture volume is given by

$$e = \sum_{i=1}^N \lambda_i e_i(p, v_i), \quad v = \sum_{i=1}^N \lambda_i v_i(p, T), \quad (1)$$

where λ_i are the component mass fractions. The EOS forms in equation (1), (absent component interaction terms), are the ones most often used and define the EOS for the mixture in terms of the partial volumes of the components, that in turn depend on the temperature and pressure of the mixture.

When modeling explosive materials by real (i.e., non-linear) equations of state, the solution of the above equations requires a pressure and temperature equilibration algorithm for a specified energy and composition of the mixture, that we will refer to as p, T -equilibration. The residuals to determine pressure, temperature equilibrium, at fixed composition are specified in equations (2),

$$\begin{aligned} F_1 &= e - \sum_{i=1}^N \lambda_i e_i(p, v_i) = 0 \\ F_2 &= v - \sum_{i=1}^N \lambda_i v_i(p, T) = 0. \end{aligned} \quad (2)$$

The expressions are nonlinear and convergence to a solution state requires the user to provide a guess for p and T as a seed value for an iterative algorithm. As part of the solution process, the partial volumes $v_i(p, T)$ must be determined as single-valued. But depending on the EOS form, the partial volumes are not necessarily single-valued and convergence to a root is not always guaranteed when using non-linear root finding algorithms. The cause of lack of con-

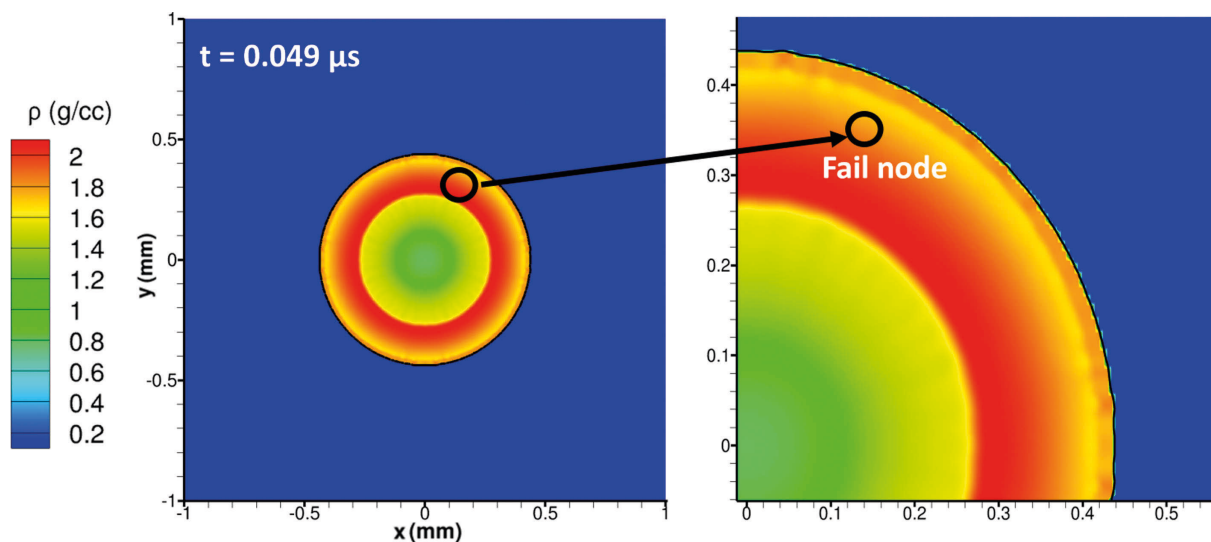


Figure 2. The image shown for the HMX example is a density pseudo-color plot at $t = 0.049 \mu\text{s}$, and marks the point where failure occurs in the simulation. The states at the fail node are: $v = 0.5996 \text{ cc/g}$, $e = 0.1073 \text{ kJ/cc}$ and $\lambda = 0.014$.

vergence is mainly due to poor initial seed guesses or non-existence of a solution. Another possibility is that values of pressure and temperature may converge to states that are physically unacceptable even though the pressure and temperature are otherwise positive.

3 Simulation Failure Traced to Models for the Component Equations of States

We present two examples of code failure that can be traced to inadequacies of the equation of state. In both cases the two-component model with the EOS forms had been calibrated and used successfully for detonation simulations [1,6], but were subsequently found to exhibit serious difficulties, especially at lower pressures. In both examples the computational domain was a $2 \text{ mm} \times 2 \text{ mm}$ square box with a 0.4 mm radius cylindrical disk. A 0.2 mm radius hot spot was placed at the center of the disk to initiate a detonation event. The numerical resolution was $dx = 0.005$ and used the hydrodynamic solver described by Hernández *et al.* [11] and in Hernández's thesis [12]. An ideal EOS was used for inert air with a density of 0.02 g/cc .

In the first example a circular disk of HMX is ignited by a hotspot placed at the center of the domain. The John Wilkins Lee (JWL) EOS form and a simple pressure based rate law proposed by Lambert *et al.* [6] was used for both reactant and products. The calibrated EOS and rate law parameters are listed in the Appendix. The initial, pressure, density and temperature for the explosive were $10\text{--}4 \text{ GPa}$, 298.18 K and 1.835 g/cc respectively. The initial hot spot pressure, temperature and density were 41.67 GPa , 3888.2 K and 2.5413 g/cc . The initial particle velocity was set to zero. The high pressure, temperature hot spot expanded radially,

and quickly an outward expanding detonation wave was formed as HMX reactants are consumed.

The simulation progresses in a seemingly consistent way, but as the pressure starts to drop it suddenly fails in a region away from the air/explosive interface where the predicted states seem otherwise physical. Figure 2 identifies the density, one time step just before failure. The circled point shows the location of the failed state point in the next time step. The pressure and sound speed fields right before failure are shown in Figure 3 and appear to be physically acceptable states. The pre-failure (last computed) values at the subsequent failed point were $v = 0.5996 \text{ cc/g}$, $e = 0.1073 \text{ kJ/cc}$ and $\lambda = 0.014$, which are physically acceptable values. When the simulation fails, one discovers that the pressure temperature equilibration of the reactants and products failed to converge to a root. Further analysis shows that at this point the partial volume nonlinear solve for the reactants in particular, fails to find a root within a specified tolerance. Failed estimates of the pressure and temperature, computed as part of the iterative Newton-Raphson method at the instance of failure were 281.6 GPa and 11068 K , which are outside physical acceptable values for reactants.

The second example consisted in the same experimental setup as before but we replaced HMX with TATB and used the Wide Ranging EOS [1] instead of the JWL EOS. Similar failure behavior was observed in this example. We do not provide the fail state values but discuss reasons behind failure in the next section (both examples exhibit the same type of issues and behaviour).

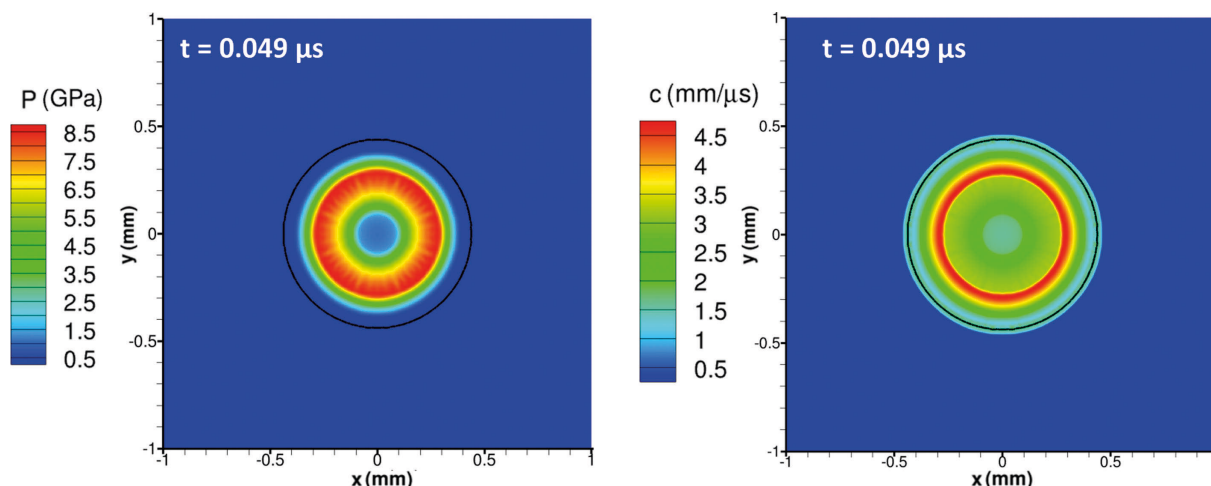


Figure 3. The image shows the HMX example pressure and sound speed pseudo-color plots when failure occurs in the simulation.

3.1 Generic Occurrence of Multiple or no Roots for Pressure, Temperature Equilibrium Closure

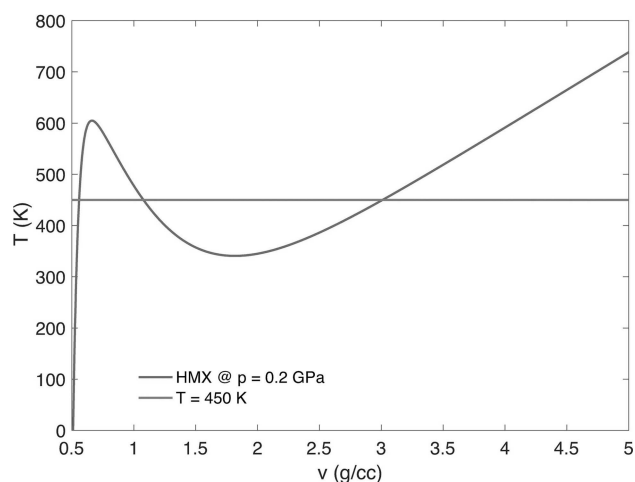
The failure of the simulation described above, is a generic occurrence and is commonly encountered by users of explosive simulation codes. The cause of the (generic) failure can be traced to the EOS forms (such as the JLW form, or the more recently used Wide Ranging (WR) EOS form) used to model real explosive components. To illustrate this difficulty we computed the temperature as a function of volume at different constant pressures for HMX and TATB. The HMX JWL EOS forms used in the Ignition and Growth models, and TATB WR EOS forms, are the same those used in Stewart *et al.* [4] and Wescott *et al.* [1], (with the modifications made by Aslam [13]) respectively, and are listed in the Appendix. Figure 4(a) shows the reactant temperature as function of reactant specific volume for HMX, for the JWL EOS at 0.2 GPa. At 450 Kelvin three roots are found. Figure 4 (b) shows the reactants volume at 5 GPa and shows a single root at 2500 K. Likewise, Figure 5(a) shows data for TATB using the Aslam-modified reactants WR EOS at 0.5 GPa, with two roots indicated at 1000 K. Figure 5(b) shows data for TATB using the Aslam-modified reactants WR EOS at 5 GPa, again with two roots indicated at 1000 K. The examples (for pressure and temperatures that could be realized in an application) show that the ill-posed functional EOS forms can lead to failure to find physically based solutions and can be the cause of unstable behavior and failure in multi-component reactive hydrodynamic solvers. For the two representative cases, (typical) explosive simulations are well behaved so long as the material is at high pressure and temperature states that are relatively close to the shock Hugoniot, or to complete reaction Hugoniot states used to calibrate the component EOS forms in regions where the pressure, temperature volume are regular. However the pressure temperature regions around the shock and complete reaction Hugoniot states for detonation, represents a

very limited portion of the state space that explosive material may experience in an application.

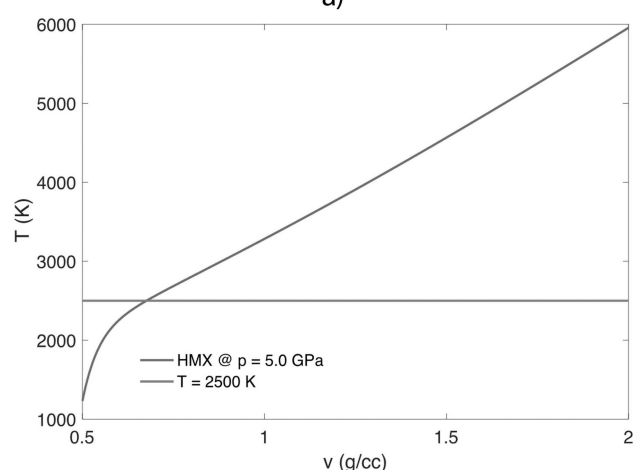
In particular, the reactants EOS forms that are commonly used have complete equation of state forms that generate specific volume, pressure and temperature EOS that may be thermodynamically ill-posed. Either the specific volume is not defined in physically admissible regions of pressure and temperature, or have volumes that lie above (are greater than) those of the products, for the same pressures and temperatures. For example, Figure 6(a) shows a typical problem encountered for certain implementation of the Ignition and Growth models that use JWL EOS reacted and unreacted Hugoniot, here shown for our HMX case. Figure 6(b) shows the $v(p, T)$ surface. It is clear that above the intersection point the $p - v$ plot is unphysical; the unreacted Hugoniot lies above the complete reacted Hugoniot. Note that development of the WR EOS introduced by Wescott *et al.* [1], was motivated as a means of fixing this problem with the shock and complete reactant Hugoniots.

By “unphysical” we restrict our comments to a two component model, where at a given thermodynamic state in pressure and temperature, the specific volume of the products is presumed to be larger than those of the reactants. If one has many more components then the thermodynamic possibilities have not been analysed in any systematic way that we know of. One can view our assertion as a modelling recommendation. See reference [14] for a recent calculation with many components enabled by CHEETAH.

Suppose we use the WR EOS forms to replace the JWL forms for the same explosive HMX. The Appendix lists the parametrization of the WR EOS forms for HMX. Figure 7(a) shows the corresponding Hugoniots curves for HMX that seem physically acceptable WR EOS forms for the reactants and products EOS. But on closer examination, Figure 7(b), shows a region of pressure and temperature values that lead to an unphysical situation where for the same pressure and temperature, the products volume is smaller than the



a)

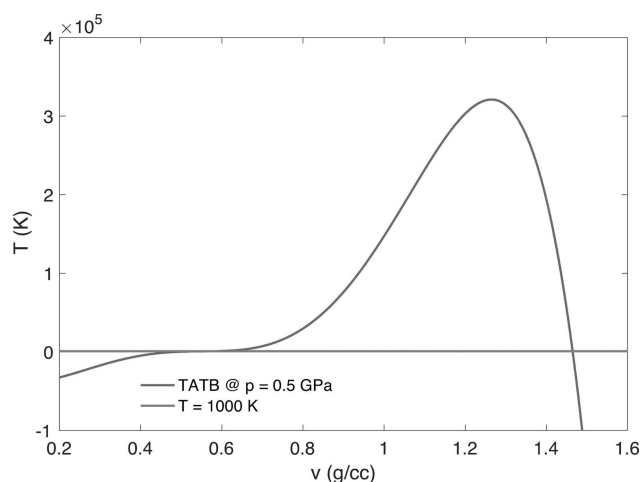


b)

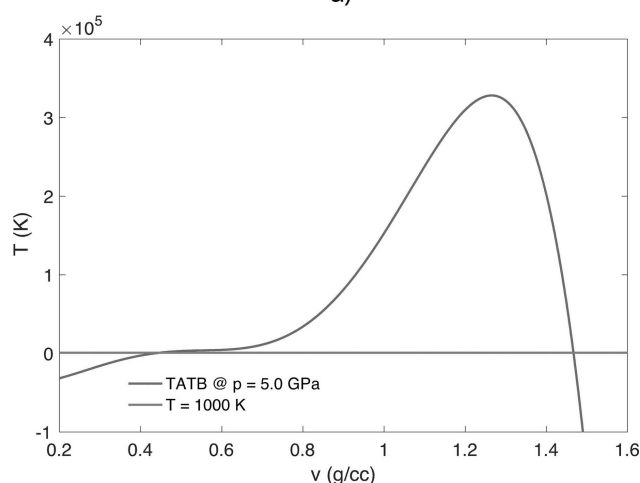
Figure 4. Shows temperature as a function of volume for HMX for the JWLL reactants EOS at (a) pressure of 0.2 GPa and (b) 5 GPa. In (a) at 450 K the reactants volume has three roots while in (b) there is a single root.

reactants volume. Numerically, this is problematic for the $p - T$ equilibrator, since it can sample p and T states in this unphysical region as part of the root solving process. Typical hydrocode related errors due to EOS issues that arise are the occurrence of negative pressures ($p < 0$), negative temperature ($T < 0$), that lead to negative sound speeds, or very large temperature/pressure spikes. During a simulation this leads to a code stop.

When this problem is encountered practitioners often force the code to continue to run and use an ad hoc, on the fly fix that “patches the states” when points with unphysical values are encountered. For example, if $p < 0$, set $p = p_0$ where p_0 is some reference minimum pressure. Such ad-hoc fixes cover up the underlying difficulty and abandon more physically based approaches. In particular, since there is no physically based estimate of the bulk temperature in the mixture, it is impossible to make sensible models of chem-



a)



b)

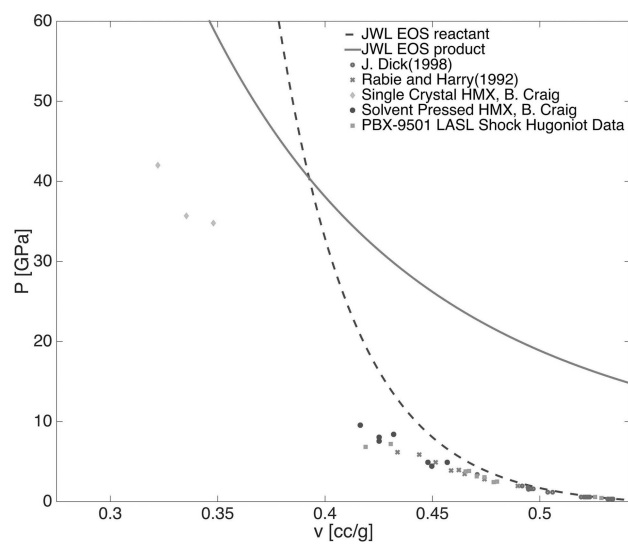
Figure 5. Shows temperature as a function of volume for TATB using the WR reactants EOS at (a) pressure of 0.5 GPa and (b) 5 GPa. In both (a) and (b) the volume has two roots for the temperature range shown.

ical reaction rates with attendant improvements as more chemical complexity is introduced into the models for reactive flow.

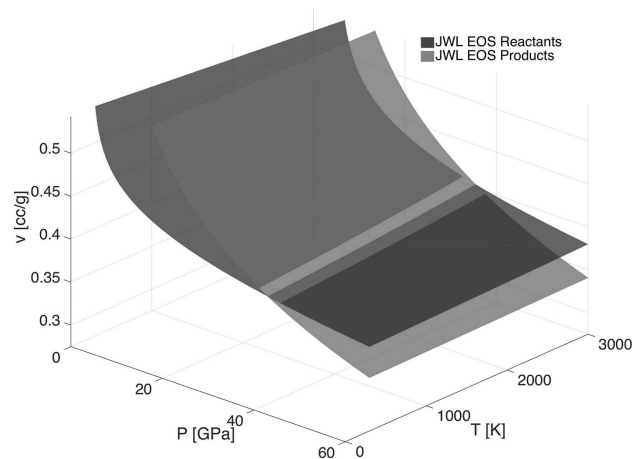
4 Consistent Equations of State

To improve the modeling of explosive systems, better EOS forms must be used that correspond to consistent thermodynamic properties in the explosive performance space. To this end the following model objectives need to be achieved:

1. Improved thermodynamic properties in the explosive performance state space.
2. Monotonically increasing energy and volume surfaces.
3. Wider admissible for the $v(p, T)$ and $e(p, T)$ functions.

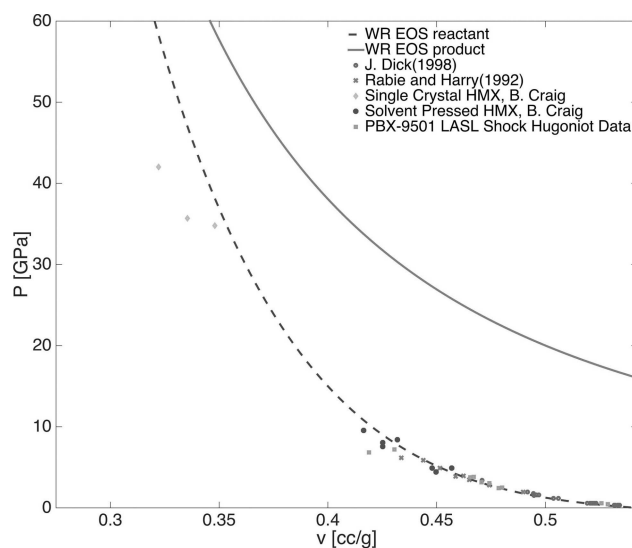


a)

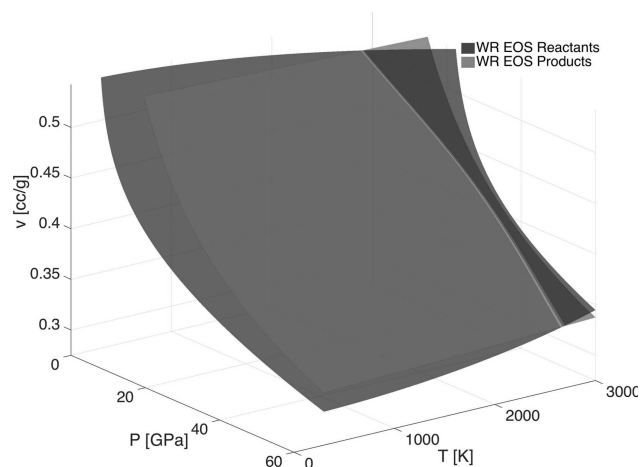


b)

Figure 6. HMX using the JWL EOS. (a) Shows reacted and un-reacted Hugoniot curves (b) $v(p, T)$ surface plot.



a)



b)

Figure 7. HMX using the WR EOS. (a) Shows reacted and un-reacted Hugoniot curves (b) $v(p, T)$ surface plot.

4. Take full advantage of modern Molecular Dynamics (MD) and Reactive MD (RMD) [6] information and simulation.
5. New forms must predict all the previously experimental data routinely used in calibration such as shock Hugoniot data.

For the current discussion, we considered four fitting forms: JWL, WR, Fried-Howard Gibbs EOS (FHG) and a Hydrostatic Thermoelastic Solid (HTES) EOS. A complete equation of state for the individual components and mixture was enforced. Three of the four, JWL, WR and FHG are found in the literature. The HTES form is a simple extension of a linear thermoelastic equation of state in the hydrostatic limit (i.e., the stress tensor is represented by the pressure and the stress state is dilatational). The Appendix gives the complete EOS forms, with the constants of the parameter-

ization. Ignition and Growth models use the JWL for both the reactants and products. The WR EOS has one EOS form for the reactants, and a different form for the products. The FHG form has been used mainly for reactants but was originally developed modeling solid and liquid carbon. The HTES form can be used to model low pressure reactants.

Next we discuss how these different forms can be used in a thermodynamically consistent way over the expected operational range of pressure and temperature states experienced by the explosives. Any of the forms listed above (or other EOS forms, such as those listed by Davis in Chapter 3 of "Explosive Effects and Applications" [15]), can be used for either the reactant or product equation of state. The only requirement is that the form be sensibly calibrated to avail-

able data, and that the forms chosen are analytically or computationally tractable. These same forms can be used to create tabular equations of state. Thermodynamic consistency means that the state variables are defined in physical regions and that the thermodynamic variables have sufficient continuity and smoothness.

4.1 Aside: Tabulated Volume, Pressure, Temperature Surfaces

If one considers the pressure, temperature and composition as the primitive physical thermodynamic states, the thermodynamic surfaces can be derived from the Gibbs potential, in particular. Tabular volume, pressure temperature surface representations can be used to enable faster non-linear iterative solves for $p - T$ equilibration once the basic thermodynamic choices for the components are established.

As part of the $p - T$ equilibration process, the partial volumes, v_i , need to be determined. In the FHG EOS, specific volume is an explicit function of pressure and temperature, hence partial volumes are determined by simply evaluating the $v_i(p, T)$ EOS form; while for the WR and JWL EOS volume is nonlinearly dependent on pressure and temperature. Convergence and monotonicity of the inversion will depend on the EOS used and is not always guaranteed. For this reason, $v(p, T)$ tabular data is generated by pre-computing the volume and removing unphysical solution branches ensuring monotonicity. A table is created by numerically inverting any required functions since equation of state forms do not necessarily lend themselves to the required explicit form. This is done for both the reactant and products and is a method used for representation used by thermodynamic equilibrium programs like CHEETAH [16].

For example, replacing v in equation (A10) in the products EOS form (A16) leads to residual in v , parameterized by p and T as,

$$f = p - p_p^s(v) - \frac{C_v \Gamma_p}{v_p} (T - T_p^s(v)). \quad (3)$$

A Newton/bisection method is used to drive the residual towards zero until convergence, for the root for v . One can populate the table for $v(p, T)$ in a minimum and maximum range (i.e., here we set pressure range is from 10–4 GPa to 80 GPa and temperature from 10 K to 15000 K). Values of p , T related to non-converging solutions in un-physical regimes should be excluded from the table. The table provides values of v given p , T by means of table bilinear interpolation. Higher accuracy can be achieved by introducing more sample points to the tables and by using higher order interpolation schemes.

4.2 Example of How to Make Consistent Improvements to the Component EOS Forms

Next we illustrate how eliminate the difficulties discussed in Section 3.1 for the same explosive material, HMX. In particular, we retain the WR products EOS form, but replace the WR reactants EOS form with the FHG EOS form. The WR EOS was already well-calibrated to complete reaction Hugoniot data and thus was not changed. The FHG EOS for the reactants was calibrated to match the shock Hugoniot data for HMX. Figure 8(a) shows the revised HMX model component surfaces for the volume, pressure temperature surface. Figure 8(b) shows the revised HMX model component surfaces for the specific internal energy, pressure and temperature surfaces. One should compare Figure 8(a) with Figure 7 and note that the (revised) FHG reactants component volume is always lower than the component products

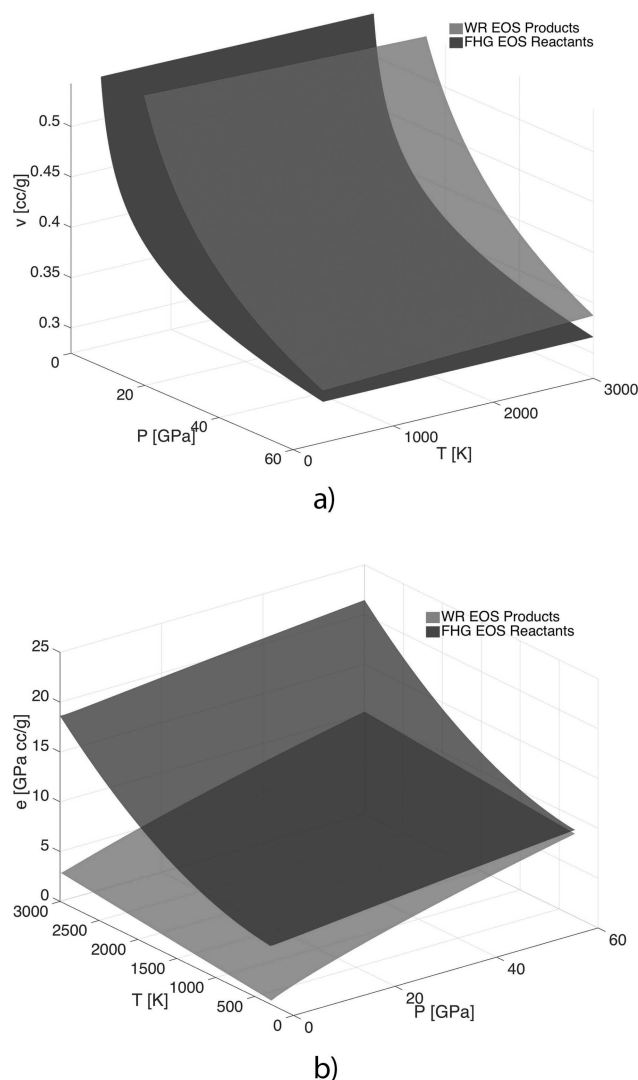


Figure 8. (a) Shows $v(p, T)$ volume surfaces and (b) $e(p, T)$ energy surfaces for HMX reactants and products.

for the same pressure and temperature. Figure 9 shows the $p - v$ and $U_p - U_s$ Hugoniot curves respectively and shows good to excellent matches to the experimental shock data.

4.3 Example of Improved (Non-failing) Simulation with Revised EOS Forms

Finally, we revisit the example problem discussed in Section 3.1 for HMX, where the product component was modeled with the WR EOS form, and the reactants was also modeled with the WR EOS form. Revisions were made to

the reactants EOS, as discussed in the last section and the reactants EOS was replaced with the FHG EOS form. The simulations were then carried out with the same initial conditions described in Section 3.1 and no instability, or loss of solution were observed. Figure 10 shows the results of the same simulation described in Section 3, but use the FHG EOS forms for the reactants. The simulation now proceeds smoothly and encounters no difficulties as the reactants are consumed and the products expand into a larger volume. Figure 10 shows the results of simulation at the much later time, $t = 0.26 \mu\text{s}$.

5 Conclusions

In order to improve predictive models for explosive performance, we advocate always using a consistent thermodynamic framework that describes the components in the material. This is essential to enable systematic modeling of realistic, temperature dependent chemistry in the reaction zone. Consistency requires complete equations of states used for each component at the minimum. We showed how commonly used, state of the art models running real material simulations will stop or exhibit “strange” behavior when the explosive products and reactants pressure and temperature develop negative pressures that lead to estimates of negative sound speed, etc. Poorly posed EOS forms lead to multiple solutions for partial component volumes in particular, and that is likely the most commonly encountered issue. A set of related techniques to make the model consistent and computationally efficient include more or less standard techniques such as the creation of tabular equation of states, but should be generated from complete equations of state. Exothermic products should generally have larger volume than their reactants at the same pressure and temperature. We presented a carefully developed example that showed that careful attention to the EOS forms for a simple 2-component reactive flow model can resolve the inherent difficulties that are encountered when ad hoc or ill-posed model EOS forms are used to compute detonation flows out of range of their calibration. The ability of a reactive flow model to replicate all standard diagnostic experiments is essential requirement.

Appendix A: EOS Forms for Components

A.1 Jones Wilkens Lee (JWL) EOS

The JWL EOS form for components is used for both the reactants and products in the I&G model. A consistent thermal and mechanical EOS for a component is equivalent to the complete equation of state. The JWL thermal EOS is described by,

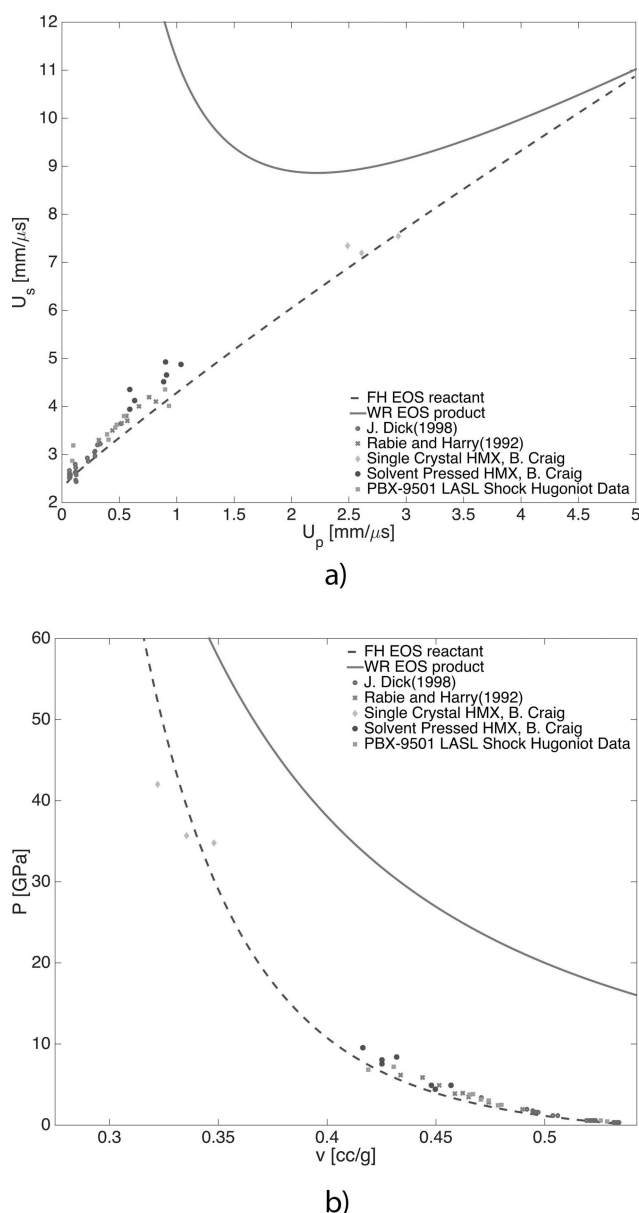


Figure 9. (a) $U_p - U_s$ Hugoniot and experimental data[17,21,22] and (b) $p - v$ Hugoniot and experimental data for HMX reactants and products.

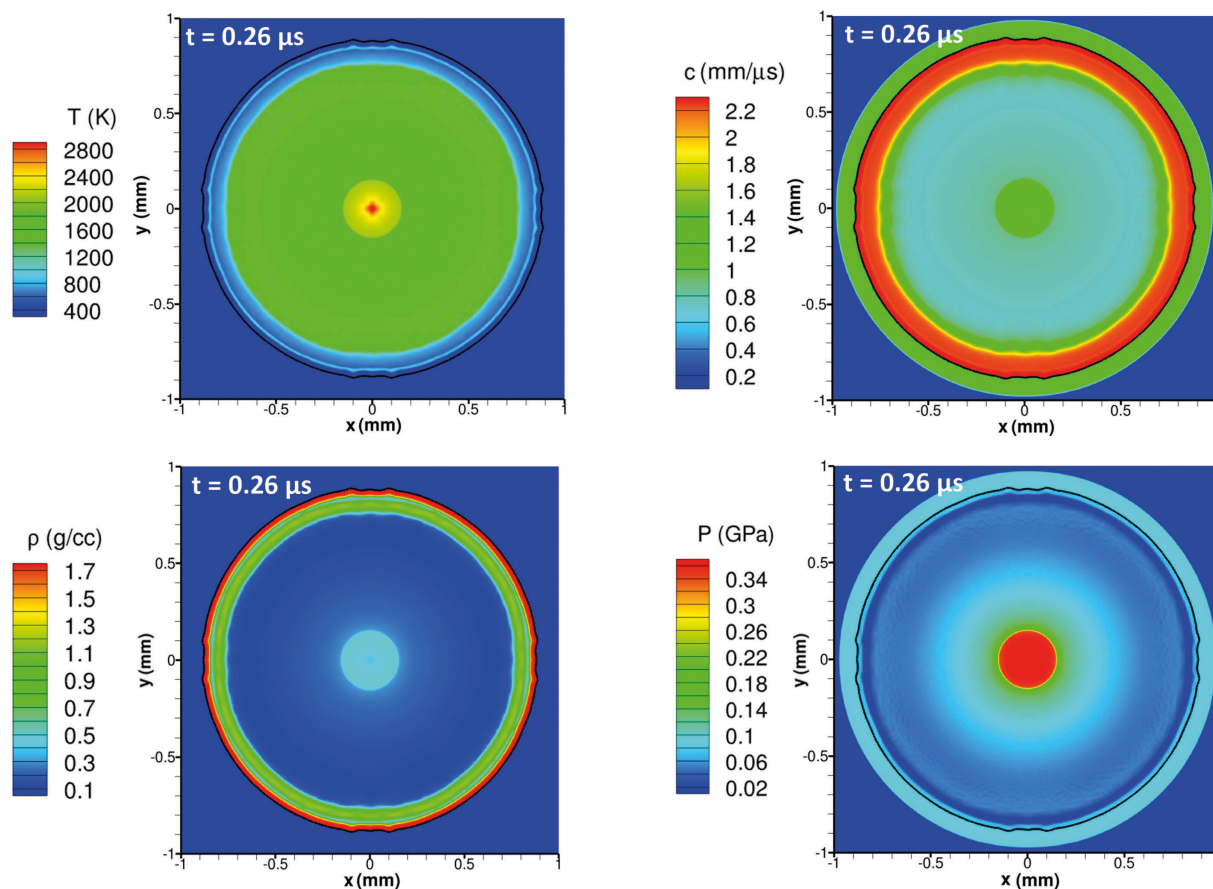


Figure 10. HMX expanding disk problem density, pressure, sound speed and temperature pseudo-color plots at 0.26 μs after using the WR products and FHG reactants EOS model.

$$p = A_i e^{-R_{1i} V_i} + B_i e^{-R_{2i} V_i} + \frac{\omega_i C_{vi} T}{V_i} \quad (\text{A1})$$

and the mechanical EOS by,

$$\frac{e_i}{v_0} = \frac{p V_i}{\omega_i} + A_i \left(\frac{1}{R_{1i}} - \frac{V_i}{\omega_i} \right) e^{-R_{1i} V_i} + B_i \left(\frac{1}{R_{2i}} - \frac{V_i}{\omega_i} \right) e^{-R_{2i} V_i} + \frac{e_{0i}}{v_0} \quad (\text{A2})$$

where A_i , B_i , R_{1i} , R_{2i} , ω_i and C_{vi} are the individual phase EOS constants, e_{0i} is the reference energy, with $E_{0i} = \frac{e_{0i}}{v_0}$ and $V_i = \frac{v_i}{v_0} = v_i/v_0$ with $i = r$ for reactants and $i = p$ for products. $v_0 = \frac{1}{\rho_0}$ is the specific volume of the original, unshocked mixture. The standard I&G calibration choose the value of Br so that when $p = p_0$, $T = T_0$.

A.1.1 JWL Parameterization for HMX

Table 1 lists the JWL EOS parameters [4]. Table 2 lists the parameters for the simple pressure based rate law [6], given

Table 1. JWL parameters for HMX.

	Reactants	Products
A (GPa)	952200.	1668.9
B (GPa)	−5.944	59.69
R_1	14.1	5.9
R_2	1.41	2.1
C_v (GPa/K)	2.7806×10^{-3}	1.0×10^{-3}
ω	0.8938	0.45
E_0 (GPa)	0.0	−10.2
V_0 (cc/g)	0.54496	0.54496

Table 2. HMX simple rate law parameters.

p_{CJ} (GPa)	k (μs^{-1})	N	ν
36.3	110	3.5	0.93

by equation (A3) where ν is the depletion exponent, p_{CJ} is the pressure at the Chapman-Jouguet point, N is the pressure exponent and k is the rate constant. This rate law was used for the example calculations shown in Section 3.

$$r = k(1 - \lambda)^{\nu} \left(\frac{p}{p_c} \right)^N \quad (\text{A3})$$

A.2 Wide Ranging (WR) EOS

The Wide Ranging EOS (WR) is based on complete equations of state developed by Davis, with modifications by Stewart *et al.* [5], and was used for predictive simulations by Lambert *et al.* [6], and in Wescott *et al.* [1]. The WR EOS forms are different for the reactant and product component.

A.2.1 WR Reactants

The mechanical EOS is given by

$$p = p_r^s(v) + \frac{\Gamma_r(v)}{v} [e - e_r^s(v)] \quad (\text{A4})$$

with the pressure on the principle isentrope given by

$$p_r^s(v) = \hat{p} \left[\sum_{j=1}^3 \frac{(4By)^j}{j!} + C \frac{(4By)^4}{4!} + \frac{y^2}{(1-y)^4} \right], \quad (\text{A5})$$

with $y = 1 - \frac{v}{v_0}$ and $\hat{p} = \frac{\rho_0 A^2}{4B}$. The constants A and B are chosen to fit experimental shock Hugoniot data. Gruniesen gamma Γ_r is given by

$$\Gamma_r(v) = \Gamma_r^0 + Z\gamma \quad (\text{A6})$$

The thermal equation of state is given by

$$T_r = T_r^s(v) + \frac{e - e_r^s(v)}{C_v} \quad (\text{A7})$$

$$T_r^s(v) = T_0 e^{-Z\gamma} \left(\frac{v}{v_0} \right)^{-\Gamma_r^0 + Z} \quad (\text{A8})$$

Where on Equation (A8) the e is an experimental, α_{st} is a constant used to calibrate the shock temperature, and C_v^0 is obtained from the thermodynamic relationship,

$$C_v^0 = C_p(1 + \beta\Gamma T)^{-1} \quad (\text{A9})$$

A.2.2 WR Products

The mechanical EOS for products is given by

$$p = p_p^s(v) + \frac{\Gamma_p(v)}{v} [e - e_p^s(v)] \quad (\text{A10})$$

The principle isentrope $p_p^s(v)$ and energy $e_p^s(v)$ are given by

$$p_p^s(v) = p_c \frac{\left[\left(\frac{v}{v_c} \right)^n + \left(\frac{v}{v_c} \right)^{-n} \right]^{\frac{a}{n}}}{\left(\frac{v}{v_c} \right)^{k+a}} \frac{k-1+F(v)}{k-1+a} \quad (\text{A11})$$

$$F(v) = \frac{2a \left(\frac{v}{v_c} \right)^{-n}}{\left(\frac{v}{v_c} \right)^n + \left(\frac{v}{v_c} \right)^{-n}} \quad (\text{A12})$$

$$\Gamma_p(v) = k-1 + (1-b)F(v) \quad (\text{A13})$$

$$e_p^s(v) = e_c \frac{\left[\left(\frac{v}{v_c} \right)^n + \left(\frac{v}{v_c} \right)^{-n} \right]^{\frac{a}{n}}}{\left(\frac{v}{v_c} \right)^{k-1+a}} \quad (\text{A14})$$

$$e_c = \frac{p_c v_c}{k-1+a} \quad (\text{A15})$$

where p_c , v_c , a , k , n , and b are used to calibrate the experimental data. The thermal EOS form is then given by

$$T_p = T_p^s(v) + \frac{e - e_p^s(v)}{C_v} \quad (\text{A16})$$

where the temperature on the principle isentrope is

$$T_p^s(v) = T_c \frac{\left[\left(\frac{v}{v_c} \right)^n + \left(\frac{v}{v_c} \right)^{-n} \right]^{\frac{a}{n}(1-b)}}{\left(\frac{v}{v_c} \right)^{k-1+a(1-b)}} \quad (\text{A17})$$

Where

$$T_c = \frac{2^{-\frac{ab}{n}} p_c v_c}{k-1+a} \quad (\text{A18})$$

Details on the WR product calibration procedure are found in Wescott *et al.* [1]. Table 3 gives the parameterization of the EOS forms used for the example shown in Section 3. The simple rate law given by (A3) and Table 2 was used with the WR EOS forms. The WR EOS forms for reactants for TATB explosive, shown in Figure 5 use the parameters list in Table 4.

Table 3. HMX WR parameters.

Reactants		Products	
Z	−0.03076	a	0.7965
B	2.737	n	1.758
C	1.45	b	0.7
Γ_0	0.7989	k	1.3
A	2.339	v_c	0.8314
α	0.6944	p_c	3.738
c_{v_r}	0.001088	c_{v_p}	0.000945
e_{0_r}	0.	e_{0_p}	−5.85

Table 4. PBX-9502 WR reactants.

Reactants	
Z	0.0
B	4.6
C	0.34
Γ_0	0.56
A	1.8
α	0.4265
c_{v_r}	0.001074
e_{0_r}	0.

A.3 Fried-Howard Gibbs (FHG) EOS

The Explicit Gibbs Free Energy equation of state of Fried and Howard [18] was originally derived for modeling solid and liquid carbon. This EOS provides a closed form for the Gibbs free energy $g(p, T)$, where thermodynamic properties may be easily derived and was shown to be consistent with more recent literature. The Gibbs free energy is separated into a “reference” term, $g_0(p, T)$, which describes properties at the reference pressure p_0 and an “equation of state” term,

$$g(p, T) = g_0(p, T) + \Delta g(p, T) \quad (\text{A19})$$

The “reference” term is computed by the following expression,

$$g_0(p, T) = \tilde{h}_0(T) - T\tilde{s}_0(T) \quad (\text{A20})$$

where the function $\tilde{h}_0(T)$ and $\tilde{s}_0(T)$ are expressed in terms of the heat capacity at constant pressure,

$$\begin{aligned} \tilde{h}_0(T) &= h_0 + \int_{T_0}^T c_{p,0}(T) dT, \\ \tilde{s}_0(T) &= s_0 + \int_{T_0}^T \frac{c_{p,0}(T)}{T} dT \end{aligned} \quad (\text{A21})$$

here h_0 and s_0 are the heat of formation and entropy respectively. After using the sum of two Einstein oscillators and a linear expression for $c_{p,0}(T)$ [19] the entropy and heat of formation are expressed as,

$$\begin{aligned} \tilde{h}_0(T) &= h_0 + \sum_{i=1}^2 a_i \left[\frac{1}{e^{x_i} - 1} \right]_{x_0}^{x_i} \\ &+ a_3 (T^2 - T_0^2) \end{aligned} \quad (\text{A22})$$

$$\begin{aligned} \tilde{s}_0(T) &= s_0 + \sum_{i=1}^2 a_i \left[\frac{x_i}{e^{x_i} - 1} - \ln(1 - e^{-x_i}) \right]_{x_0}^{x_i} \\ &+ a_3 (T - T_0) \end{aligned} \quad (\text{A23})$$

where $x_i = \frac{\theta_i}{T}$ and $x_0 = \frac{\theta_i}{T_0}$.

For the “equation of state” term Fried and Howard [18] found that the generalized Murnaghan form of Equation (A24) to compute the specific volume was more accurate for conditions of elevated pressure and temperature. This form assumes that the bulk modulus, B , is a linear function of pressure, $B = B_0 + np$ where $B_0 = \frac{1}{\kappa_0}$.

$$v(p, T) = v_0 [n\kappa_0 p + f(T)]^{-\frac{1}{n}} \quad (\text{A24})$$

With

$$f(T) = e^{-n[f_a(T) - f_a(T_0)]} \quad (\text{A25})$$

where

$$f_a(T) = \alpha_0 T + \alpha_1 \left[T - \frac{T^*}{2} \left(e^{-\frac{T}{T^*}} - 2 \right)^2 \right] \quad (\text{A26})$$

The “equation of state” term, $\Delta g(p, T)$, is finally expressed as,

$$\Delta g(p, T) = \frac{v_0}{(n-1)\kappa_0} [\eta^{n-1} - \eta_0^{n-1}] \quad (\text{A27})$$

where

$$\eta = \frac{v_0}{v} = [n\kappa_0 p + f(T)]^{\frac{1}{n}} \text{ and } \eta_0 = \eta(p_0, T) \quad (\text{A28})$$

Given $g(p, T)$ and $v(p, T)$ the internal energy is easily found by,

$$\begin{aligned} e(p, T) &= h_0 + \int_{T_0}^T c_{p,0}(T) dT \\ &+ \frac{v_0}{(n-1)\kappa_0} [\eta^{n-1} - \eta_0^{n-1}] \\ &- \frac{v_0}{n\kappa_0} T f'(T) [\eta^{-1} - \eta_0^{-1}] \\ &- p v_0 [n\kappa_0 p + f(T)]^{-\frac{1}{n}} \end{aligned} \quad (\text{A29})$$

where

Table 5. HMX FHG EOS reactant parameters.

v_0 (cc/g)	κ_0 (GPa $^{-1}$)	n	α_0 (K $^{-1}$)	α_1 (K $^{-1}$)	T^* (K)
0.5423	0.095	6.8	-3.0×10^{-4}	3.329×10^{-4}	100.0

Table 6. HMX FHG EOS reference state parameters.

h_0 (GPa cc/g)	$\frac{a_1}{R}$	$\frac{a_2}{R}$	$\frac{a_3}{R}$ (K $^{-1}$)	θ_1 (K)	θ_2 (K)
5.85	6.124	0.174	0.09835	0.2788	0.534

$$c_{p,0}(T) = \sum_{i=1}^2 a_i \frac{x_i^2 e^{x_i}}{(e^{x_i} - 1)^2} + a_3 T \quad (\text{A30})$$

For the parameters on Table 5, κ_0 and n are within the reported ranges by Sewell *et al.* [19]; α_0 and α_1 are adjusted to avoid a convex shape in the internal energy surface for low pressure and temperature. Parameters in Table 6 are fitted using data from Hanson-Parr *et al.* [20].

Acknowledgements

Supported by the Office of Naval Research N00014-16-1-2057 (University of Illinois) and N00014-19-1-2084 (University of Florida). D. S. Stewart's efforts at the University of Florida were supported by the Air Force Research Laboratory, Munitions Directorate.

References

- [1] B. L. Wescott, D. S. Stewart, W. C. Davis, Equation of state and reaction rate for condensed-phase explosives, *J. Appl. Phys.* **2005**, *98*, 053514.
- [2] C. A. Handley, B. D. Lambourn, N. J. Whitworth, H. R. James, W. J. Belfield, Understanding the shock and detonation response of high explosives at the continuum and meso scales, *Appl. Phys. Rev.* **2018**, *115*, 011303.
- [3] P. Vitello, T. Lorenz, L. Fried, P. Souers, High Resolution Chemistry Based Modeling of LLM-105 Explosives, June 30, 2014, 15th International Detonation Symposium, San Francisco, CA, United States, July 13, 2014.
- [4] D. S. Stewart, A. Hernández, K. Lee, Modeling reaction histories to study chemical pathways in condensed phase detonation, *J. Appl. Phys.* **2016**, *119*, 095902.
- [5] D. S. Stewart, S. Yoo, W. C. Davis, Equation of state for modeling the detonation reaction zone, 12th Symp.(Intl) on Detonation, **2002**, 1–11.
- [6] D. E. Lambert, D. S. Stewart, S. Yoo, B. L. Wescott, Experimental validation of detonation shock dynamics in condensed explosives, *J. Fluid Mech.* **2016**, *546*, 227–253.
- [7] S. Han, A. C. T. van Duin, W. A. Goddard, Thermal decomposition of condensed-phase nitromethane from molecular dynamics from ReaxFF reactive dynamics, *J. Phys. Chem. B* **2011**, *115*, pp. 6534–6540.
- [8] N. Mathew, M. P. Kroonblawd, T. Sewell, Predicted melt curve and liquid-state transport properties of TATB from molecular dynamics simulations, *Mol. Simul.* **2018**, *44*, 613–622.
- [9] H. B. Callen, Thermodynamics and an Introduction to Thermostatistics, Wiley **1985**.
- [10] E. L. Lee, C. M. Tarver, Phenomenological model of shock initiation in heterogeneous explosives, *Phys. Fluids.* **1980**, *23*, 2362–2372.
- [11] A. Hernández, D. Scott, S. Lieberthal, B. Lieberthal, An explicit algorithm for imbedding solid boundaries in cartesian grids for the reactive Euler equations, *Combust. Theory Mod.* **2018**, *22*, 714–743.
- [12] A. M. Hernández, Computational Modeling of Advanced, Multi-Material Energetic Materials and Systems. PhD thesis, Theoretical Applied Mechanics, University of Illinois at Urbana-Champaign **2018**.
- [13] T. D. Aslam, The reactants equation of state for the tri-amino-tri-nitro-benzene (TATB) based explosive PBX 9502, *J. Appl. Phys.* **2017**, *122*.
- [14] Peter Vitello, Sorin Bastea, Laurence E. Fried, "Improved reactive flow modeling of the LX-17 double shock experiments," AIP Conference Proceedings **1979**, 100034 (2018).
- [15] J. A. Zukas, W. Walters, Explosive Effects and Applications (Shock Wave and High Pressure Phenomena), Springer **1998**.
- [16] Cheetah 8.0 thermochemical code, Lawrence Livermore National Laboratory, Livermore, CA 94550 <https://pls.llnl.gov/people/divisions/materials-science-division/cheetah-8.0>.
- [17] J. J. Dick, A. R. Martinez, R. Hixson, Plane impact response of PBX-9501 and its components below 2 GPa, *Los Alamos National Laboratory Technical Report*, April **1998**, LA-13426-MS, UC-741.
- [18] L. F. Fried, M. H. Howard, Explicit Gibbs free energy equation of state applied to the carbon phase diagram, *Phys. Review B* **2000**, *61*, 8734–8743.
- [19] T. D. Sewell, D. Bedrov, R. Menikoff, G. D. Smith, Elastic Properties of HMX, *AIP Conf. Proc.* **2002**, *620*, 399.
- [20] D. M. Hanson-Parr, T. P. Parr, Thermal properties measurements of solid rocket propellant oxidizers and binder materials as a function of temperature, *Journal of Energetic Materials* **1999**, *17*, 1–48.
- [21] R. L. Rabie, H. H. Harry, The Characterization of British Explosives FD16, EDC29, EDC35 and EDC37, *Los Alamos National Laboratory Report* **1992**, LA-UR-92-1928.
- [22] S. P. Marsh, LASL Shock Hugoniot Data, University of California Press **1980**.

Manuscript received: April 11, 2019
Version of record online: September 23, 2019